Anharmonic lattice dynamics and neutron-scattering spectra in bcc transition metals

T. May,* W. Müller, and D. Strauch
Institut für Theoretische Physik, Universität Regensburg, D-93040 Regensburg, Germany
(Received 25 April 1997; revised manuscript received 20 October 1997)

Anharmonic phonon-phonon coupling strengths have been derived from a simple phenomenological model potential in order to explain the characteristic phonon linewidths and lineshifts and inelastic neutron spectra of bcc metals in their high-temperature phase. The strong quasielastic scattering near $\mathbf{q}=\frac{2}{3}(111)$ and $\mathbf{q}=\frac{1}{2}(110)$ in bcc Zr and bcc Ti is actually caused by anharmonic broadening, with the lifetime of these low-frequency phonons of the order of a vibrational period. These modes which are connected to the structural phase transition from the bcc to the hexagonal or the hcp phase show the strongest anharmonic effects. The interference between one- and two-phonon neutron-scattering processes leads to an unusually strong intensity variation over adjacent Brillouin zones. [S0163-1829(98)02010-4]

I. INTRODUCTION

The phonon spectra of the group-IV and -V transition metals in their high-temperature bcc phase have been examined by extended inelastic-neutron-scattering experiments.[1–3] While the bcc phase of the group-V metals is stable, for the group-III metals this phase exists only in the upper third of the temperature region below the melting point, and for the group-IV metals the range of stability narrows to 90 K below the melting point. Therefore, neutron-scattering experiments require sophisticated experimental techniques, namely, on *in situ* grown crystals.[1]

Despite of the different electronic structure some characteristic effects are very similar for all metals in their high-temperature bcc phase. The experiments show that in the narrow region between $\frac{1}{2}(110)$ and $\frac{2}{3}(111)$ either the modes are overdamped, or there is quasielastic scattering. These effects are most important for those modes whose atomic displacements are related to the structural phase transition to the low-temperature hcp phase and the high-pressure hexagonal ω phase, respectively.[1] The energy barriers between the rather open bcc structure and the hcp and ω phases are very low, and thus the modes related to these phase transitions have low frequencies. At high temperatures the atomic displacements become large, and anharmonic effects have to be taken into account.

In addition, so-called symmetry breaking phonons in the high-temperature phase of bcc La and bcc Zr have been observed,[3,4] namely, different line shapes at equivalent $\mathbf{q}$ points in different Brillouin zones and anomalous scattering intensities in adjacent Brillouin zones. In the case of bcc Zr, for example, anharmonic effects cause an additional factor of five in the scattering intensity at $\mathbf{q}=\frac{4}{3}(111)$ as compared to the symmetrically equivalent $\mathbf{q}=\frac{2}{3}(111)$.

Within the framework of perturbation theory, the nature of interference was first elucidated by Thompson[5] who has derived the expressions for phonon lifetime, phonon frequency shift, and one- and two-phonon interference effects in the scattering cross section due to anharmonicity. Lifetime effects have been observed and calculated in K,[6] and later lifetime and interference effects have been observed in the highly anharmonic bcc He.[7] Interference makes a significant contribution to the scattering intensity in solid H and probably also in Ne.[8] In most cases perturbation theory with model anharmonicities has led to a qualitative understanding of the experimental facts. High-temperature bcc metals stimulated anew the interest in understanding theoretically the vibrational properties of strongly anharmonic crystals. Scheipers and Schirmacher[9] have presented a self-consistent theory for the dynamical one-phonon structure factor.

To obtain a picture of the potential surface, in which the atoms move, the total energy of the crystal can be plotted as a function of the normal coordinate of a phonon. This was done in frozen-phonon *ab initio* calculations,[10] and the results revealed the low-energy barrier between the different structural phases of the crystal. To understand the stability of bcc Zr, Ye *et al.*[11] have extracted the anharmonic part of the interatomic potential fitted to coupling parameters from an *ab initio* frozen-phonon calculation; from that they have calculated the anharmonic frequency shift of single phonons. Willaime and Massobrio[12] have used an N-body potential with four parameters to calculate thermal expansion, phonon dispersion and damping in bcc-Zr. Saxena *et al.*[13] derived the phonon dispersion from temperature-dependent interactions from first principles.

A different approach to the behavior of the high-temperature bcc metals is molecular dynamics. Zhang *et al.*[14] have been able to reproduce the symmetry breaking effect, i.e., the abnormal scattering intensity variation, and have obtained the different line shapes in different Brillouin zones. Gornostyrev *et al.*[15] used *ab initio* potentials with several wells to calculate ω via numerical integration of the Langevin equation and obtain a central peak and splitting of phonon peaks.

As we will show in the following, the neutron-scattering spectra observed in bcc Ti and bcc Zr can be understood within a simple anharmonic lattice-dynamical model potential. Interference terms between one and two phonon processes will be taken into account which leads to the observed symmetry breaking behavior. Preliminary accounts of parts of this work have been published before.[16,17]

II. THEORETICAL ASPECTS

We have adjusted the harmonic part of a phenomenological Born-Mayer potential

$$V(r)=V_0e^{-r/r_0} \tag{1}$$

to the experimental (high-temperature) frequencies. We emphasize that this potential contains only two parameters which are adjusted only to the quasiharmonic dispersion. We also have redone our calculations using a Morse potential

$$V(r)=D(e^{-2\alpha(r-r_0)}-2e^{-\alpha(r-r_0)}) \tag{2}$$

from which we have obtained very similar results.

From the harmonic part of the potential we have obtained the harmonic eigensolutions, i.e., the quasiharmonic phonon frequencies and eigenvectors throughout the entire Brillouin zone. From the anharmonic part of the potential and from the harmonic eigensolutions we have calculated the leading parts of the phonon self-energy $\Pi(\omega)$.[18,19] The anharmonic part of the potential can be written in terms of the harmonic phonon field operators

$$V_A=\frac{\hbar}{3!}\sum_{123} V(123)A(1)A(2)A(3) + \frac{\hbar}{4!}\sum_{1234} V(1234)A(1)A(2)A(3)A(4)+\cdots , \tag{3}$$

where the index 1 stands for a combination of the wave vector $\mathbf{q}_1$ and branch index j_1 of the phonon 1, i.e., $1 \equiv(\mathbf{q}_1,j_1)$ and $\overline{1}\equiv(-\mathbf{q}_1,j_1)$.

The anharmonic coupling coefficients $V(123)$ and $V(1234)$ are given in terms of the anharmonic derivatives of the interatomic potential and the (quasiharmonic) eigenvectors and frequencies.[18,19]

The anharmonic one-phonon properties can be obtained from the anharmonic one-phonon Green function, which is, for the phonon with quantum number 1, given by

$$G_1(\omega)=\frac{2\omega_1}{\omega_1^2-\omega^2+2\omega_1\Pi_1(\omega)} \tag{4}$$

with the phonon self-energy

$$\Pi_1(\omega)=\Delta_1(\omega)-i\Gamma_1(\omega)=\Pi_1^{(3)}+\Pi_1^{(4)}+\cdots , \tag{5}$$

where $\Delta_1(\omega)$ and $\Gamma_1(\omega)$ are the shift and damping function, respectively, with

$$\Pi_1^{(3)}(\omega)=-\frac{1}{2}\sum_{23} |V(123)|^2G_{23}^0(\omega), \tag{6}$$

$$\Pi_1^{(4)}=\sum_{2} V(1\overline{1}2\overline{2})\left(n_2+\frac{1}{2}\right), \tag{7}$$

and $G_\omega^0(23)$ is the (approximately harmonic) two-phonon Green function

$$G_{23}^0(\omega)=(n_2+n_3+1)\frac{2(\omega_2+\omega_3)}{(\omega_2+\omega_2)^2-(\omega+i\varepsilon)^2} + (n_3-n_2)\frac{2(\omega_2-\omega_3)}{(\omega_2-\omega_3)^2-(\omega+i\varepsilon)^2}, \tag{8}$$

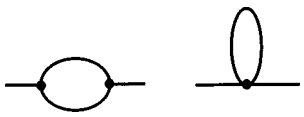

FIG. 1. Contributions $\Pi_1^{(3)}$ and $\Pi_1^{(4)}$ in Eq. (5). The first diagram leads to frequency-dependent shift and damping. The second diagram leads to a frequency-independent frequency shift.

and n_λ is the Bose occupation factor of the phonon with quantum number λ.

The contributions $\Pi_1^{(3)}$ and $\Pi_1^{(4)}$ in Eq. (5) are shown diagrammatically in Fig. 1. With the exception of thermal expansion effects we have included in Eq. (5) the effect of $V(123)$ up to second order and of $V(1234)$ up to first order. The (complex) contribution $\Pi_1^{(3)}$ describes the anharmonic decay of the phonon with quantum number 1 into two phonons with quantum numbers 2 and 3 due to third-order anharmonicity; this process has a real and an imaginary part and thus contributes both to the shift and damping function. The (real) contribution $\Pi_1^{(4)}$ describes the anharmonic coupling of the phonon with quantum number 1 to the thermal displacement fluctuations due to fourth-order anharmonicity.

In comparison with these effects the effect of thermal expansion can be neglected: With the experimentally known[1] thermal expansion coefficient of 5.144×10^{-5} Å/K a change of 100 K leads to a change of the lattice constant of 0.16%, and with the potential (1) the resulting change of the phonon frequencies is below 0.02 THz, while the effect expressed by $\Pi_1^{(3)}+\Pi_1^{(4)}$ is larger by an order of magnitude, see Sec. III C.

The model potential (1) is fitted to the experimental (anharmonically shifted, quasiharmonic) frequencies and thus contains anharmonic contributions. To correct for these contributions one must add a (real) contribution $\Pi_1^{\rm qh}$ to Eq. (5) such that the total shift function $\Delta_1(\omega_1)$ vanishes at the quasiharmonic eigenfrequency ω_1,

$$\Pi_1'(\omega)=\Delta_1'(\omega)-i\Gamma_1(\omega)=\Pi_1^{\rm qh}+\Pi_1(\omega). \tag{9}$$

In a monatomic crystal the differential cross section for one-phonon inelastic neutron scattering including the interference with two-phonon processes can be written in the form[6]

$$S(\mathbf{Q},\omega)=Nb\ \ e^{-2W(\mathbf{Q})}\sum_1 [n_1(\omega)+1] \times\sum_{\mathbf{G}} \delta_{\mathbf{Q},\mathbf{q}_1+\mathbf{G}}{\rm Im}[K_1(\mathbf{Q},\omega)K_1^*(\mathbf{Q},-\omega)G_1(\omega)], \tag{10}$$

with b the scattering length and

$$K_1(\mathbf{Q},\omega)=F_1(\mathbf{Q})-H_1(\mathbf{Q},\omega), \tag{11}$$

$$F_1(\mathbf{Q})=-i\mathbf{Q}\cdot\mathbf{e}_1\sqrt{\frac{\hbar}{2\omega_1M}}, \tag{12}$$

$$H_1(\mathbf{Q},\omega)=\frac{1}{N}\sum_{23} V(123)F_2(\mathbf{Q})F_3(\mathbf{Q})G_{23}^0(\omega). \tag{13}$$

The Debye-Waller factor $e^{-2W(\mathbf{Q})}$ leads to a decrease of the scattering intensity with increasing temperature and/or increasing scattering vector $\mathbf{Q}$ but is independent of frequency.

As in Eq. (6) the summation in Eq. (10) runs over the whole Brillouin zone, and the conservation of quasimomentum is guaranteed by the factor $\delta_{\mathbf{Q},\mathbf{q}_1+\mathbf{G}}$. The frequency dependent expression $\mathrm{Im}[\cdots]$ is weighted by the occupation number (n_1+1) and contains the one-phonon term $G_1(\omega)$, Eq. (4). $\mathrm{Im}[G_1(\omega)]$ is the resonance curve of one anharmonic phonon. $K_1(\mathbf{Q},\omega)K_1^*(\mathbf{Q},-\omega)$ contains the one- and two-phonon interference in the anharmonic case and reduces to the usual one-phonon expression in the harmonic case.

The frequency dependence of the anharmonic term $H_1(\mathbf{Q},\omega)$ modifies the line shape and intensity as compared to that given by the harmonic term $F_1(\mathbf{Q})$. This modificaton can be different in different Brillouin zones because the term H_1 depends on two factors $\mathbf{Q}$ while F_1 depends on only one factor of $\mathbf{Q}$. This leads to different line shapes in different Brillouin zones and for this reason has been called symmetry breaking behavior. It was observed in the high-temperature phase of bcc metals. Neglecting the term H_1 leads back to anharmonically damped and shifted phonons without interference with two-phonon states, and additionally neglecting of the phonon self-energy in Eq. (4) for the one-phonon Green function $G_1(\omega)$ leads to the expression for purely harmonic inelastic scattering.

III. RESULTS

A. Dispersion

The longitudinal and transverse force constants for bcc Zr are calculated with the two parameters $V_0=100$ eV and $r_0=0.6$ Å from the Born-Mayer potential (1) using the experimentally determined lattice constant $a=3.46$ Å. Figure 2 shows the resulting theoretical quasiharmonic phonon dispersion curves. There is only a narrow margin to the choice of the parameters: A change of V_0 leeds to an overall scaling of the frequencies, and only in a small region around $r_0=0.6$ Å are all frequencies real.

Interactions up to fifth-nearest neighbors have to be taken into account to stabilize the low-frequency branches. This is a well-known fact in the lattice dynamics of materials with the rather open bcc structure. Although the potential is very simple and has only two parameters it is able to give a good description of the phonon dispersion. In the case of bcc Ti we have obtained very similar results, and in contrast to the case of other fcc metals[20] there is no obvious need for angular forces. In other cases such as La and Cr the d electrons seem to stabilize the low-frequency phonons,[2,21] so that a simple central potential is not able to describe the harmonic and anharmonic properties.

In our calculations we have started from the bcc structure with real quasiharmonic phonon frequencies, and we have determined anharmonic effects within this structural phase of the crystal. In the harmonic approximation the atoms experience the low potential barriers in the directions towards the other phase structures. The resulting large amplitudes lead to strong anharmonic effects for modes with displacements in these directions.

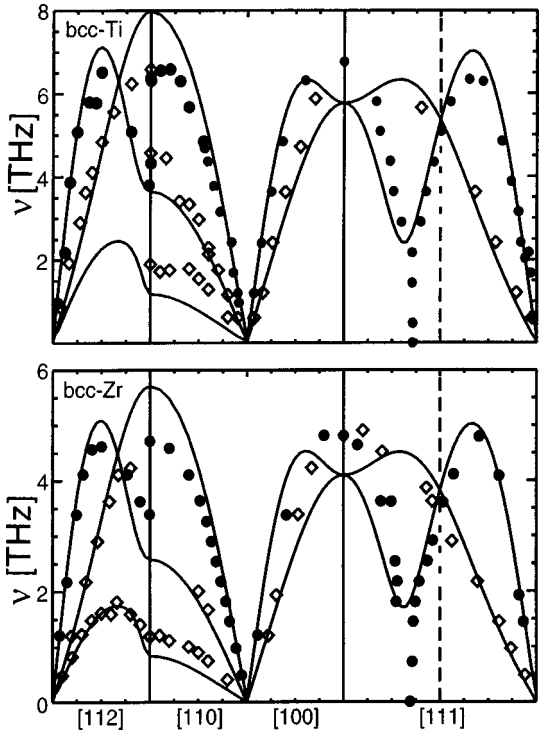

FIG. 2. Quasiharmonic phonon dispersion for bcc Ti at $T=1300$ K and bcc Zr at $T=1180$ K calculated with a Born-Mayer-potential (lines) and experimental data (Refs. 1,2) (dots).

B. Damping function $\Gamma_1(\omega)$ and linewidth $\Gamma_1(\omega_1)$

The only contribution to the damping function comes from $\Pi_1^{(3)}(\omega)$, Eq. (6). The imaginary part of $G_\omega^0(23)$ is a sum of δ functions, and we have replaced them by Gaussian functions with the same width of 0.5 THz for all phonons. This replacement is not only numerically convenient but also has the physical content of giving an averaged lifetime to the contributing phonons and of simulating resolution effects. Thus, the width of the Gaussian functions has been chosen of the order of the experimental resolution.[1]

The two-phonon Green function (8) can be written in terms of one-phonon Green functions. In a self-consistent anharmonic theory (of higher order) one would have to use anharmonic one-phonon Green functions rather than the (quasi)harmonic one-phonon Green functions, only the latter leading to the form of Eq. (8). However, there are different pairs of phonons with different widths contributing at a given frequency, and this leads to a sort of average over the different widths.

The summations in Eqs. (6) and (7) have been carried out with a cubic mesh of 1300 wave vectors distributed over the whole Brillouin zone. Convergence of the results was tested by examing different numbers of wave vectors.

Another numerical test of our results was employing the linear tetrahedron method with 631 tetrahedra in the irreducible wedge of the Brillouin zone and a mesh of 175 frequencies. The result of this test was, that for a mean phonon linewidth of 0.5 THz chosen in our calculations, the summation over the simple cubic mesh is sufficient.

The calculated damping functions $\Gamma_{\mathbf{q},j}(\omega)$ for the longitudinal branch along the [111] direction in bcc Zr at $T=1180$ K are shown in Fig. 3. Analytic properties make the damping

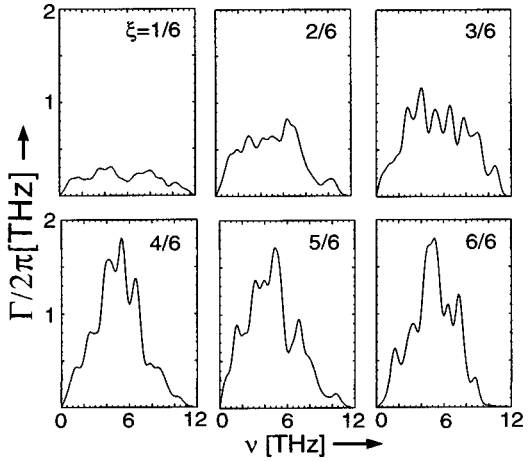

FIG. 3. Imaginary part of the phonon self-energy (damping function) $\Gamma_1(\nu)$ of Zr at $T=1180$ K for longitudinal waves with wave vector $\mathbf{q}=\xi(1,1,1)2\pi/a$.

function equal to zero at $\mathbf{q}=0$. The strongest damping occurs between $\frac{2}{3}[111]$ and the zone boundary. The damping functions become as large as the phonon frequencies, so that the low-frequency part of the branch is strongly damped.

For reasons of resolution the frequency dependence of the damping function can not be determined in the neutron-scattering experiment, but for approximately Lorentzian damping the linewidth is given by the value of the damping function $\Gamma_1(\omega_1)$ at the quasiharmonic frequency ω_1 and can be compared with experimental results, which were obtained by fitting a damped harmonic oscillator curve to the experimental line shape.[1]

A comparison of the theoretical and experimental low-frequency and strongly damped transverse T_1 [112] branch in bcc Zr at $T=1300$ K is shown in Fig. 4. Both theory and experiment show maximum damping at $\mathbf{q}=\frac{2}{3}$ [112]. In this mode the atoms move in the direction of a structural phase transition: The corresponding displacements of the atoms are symmetrically equivalent to the one of the $L\frac{2}{3}[111]$ mode and correspond to the displacement towards the transition to the ω phase.

The linewidth $\Gamma_1(\omega_1)$ for the lowest transverse branch T_1 as a function of the wave vector along the [110] direction in bcc Ti at $T=1300$ K is shown in Fig. 5. Maximum damping is found at the zone boundary, where the atomic displacements correspond to the transition towards a slightly distorted HCP phase.[1]

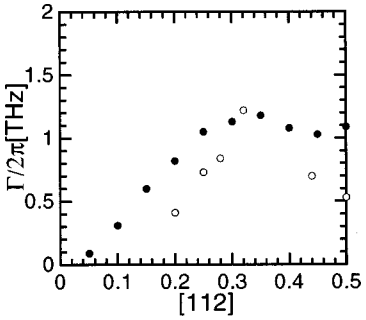

FIG. 4. Linewidth $\Gamma_1(\nu_1)$ for the transverse branch $T_1[112]$ in bcc Zr at $T=1300$ K (full symbols) in comparison with the experiment (empty symbols) (Ref. 2).

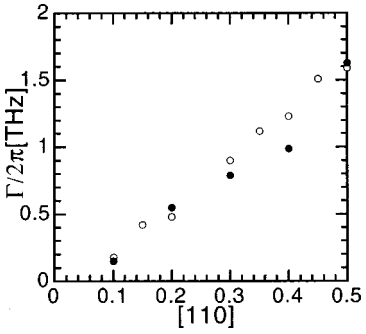

FIG. 5. Linewidth $\Gamma_1(\nu_1)$ for the transverse branch $T_1[110]$ in bcc Ti at T=1300 K (full symbols) in comparison with the experiment (empty symbols) (Ref. 1).

In all cases the theoretical values for the damping at the phonon frequencies agree very well with the experiment, although at least two approximations have been made: First, the influence of the frequency dependence of the shift function $\Delta(\omega)$ on the line shape has been neglected. As our calculations show, the modification of the line shape for low-frequency phonons is weak enough that the influence on the linewidth can be neglected. Secondly, we have neglected the interference effects on the linewidth. This is justified, because the influence of interference terms on the line shape (but not on the intensity) is small, as discussed in Sec. III E.

C. The shift function $\Delta_1(\omega)$ and line shift $\Delta_1(\omega_1)$

There are three contributions to the shift function, only one of which is frequency dependent. We have obtained the contribution $\Delta_1^{(3)}(\omega)$ which is the real part of $\Pi_1^{(3)}(\omega)$, Eq. (6), from the damping function $\Gamma_1(\omega)$ by Kramers-Kronig transform. As an example, the result for the $L\frac{2}{3}[111]$ phonon in bcc Zr at $T=1180$ K is shown in Fig. 6.

While $\Delta_1(\omega)$ is the shift function with respect to the purely harmonic frequencies, the calculation of the neutron cross section from the quasiharmonic phonon frequencies involves the function $\Delta_1'(\omega)$ as explained in connection with Eq. (9). The total shift of a quasiharmonic phonon line is given by $\Delta_1(\omega_1)$ in the case of Lorentzian behavior of the resonance. This shift from the decay process, for different symmetry directions is shown in Fig. 7. The total shift function $\Delta^{(3)}(\mathbf{q})+\Delta^{(4)}(\mathbf{q})$ shows that the contribution $\Delta^{(4)}(\mathbf{q})$

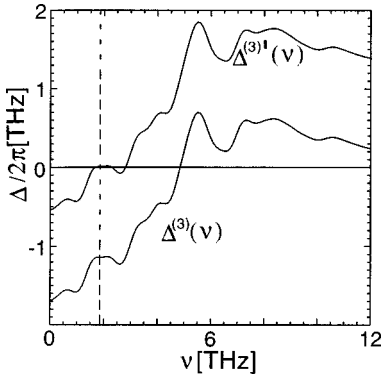

FIG. 6. Real part of the self-energy (shift function) $\Delta_1^{(3)}(\nu)$ for the longitudinal branch $L\frac{2}{3}[111]$ in bcc Zr, $T=1180$ K; for the two curves see text.

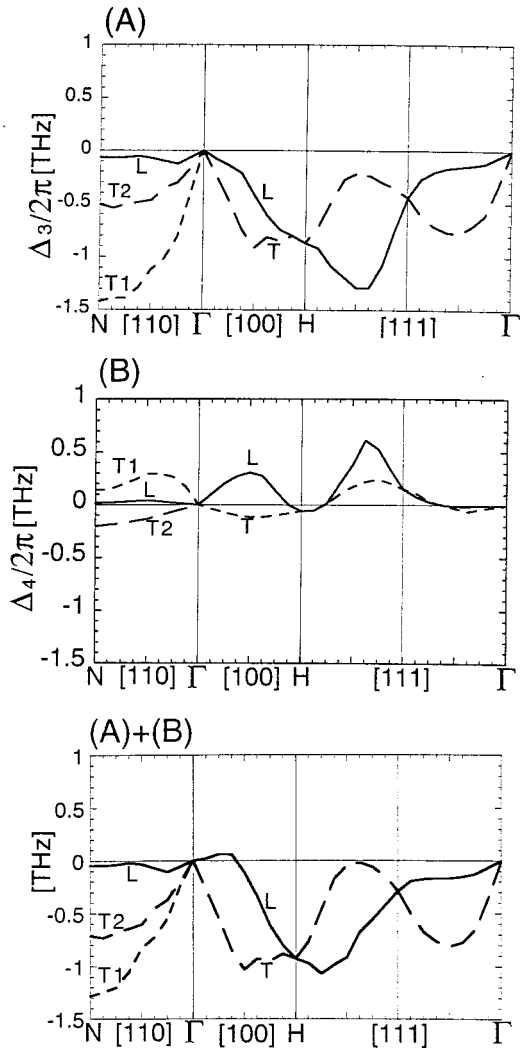

FIG. 7. Line shifts $\Delta^{(3)}(\nu_1)$ (A) and $\Delta^{(4)}(\nu_1)$ (B) as a function of wave vector **q** along the main symmetry directions in bcc Zr at $T=1180$ K. The total line shift $\Delta_1^{(3)}(\nu_1)+\Delta^{(4)}(\nu_1)$ (C).

tends to stabilize most branches, while $\Delta^{(3)}(\mathbf{q})$ leads to a general softening of the modes. Both contributions are largest for the $T[110]$ and $L\frac{2}{3}$ [111] branches. While the line shift $\Delta_1^{(4)}(\omega_1)$ is generally positive it is outweighed by the generally negative $\Delta_1^{(3)}(\omega_1)$. This is unexpected since the (total) anharmonic shift is believed to be positive and thus to stabilize the bcc structure at high temperatures. In fact, the results of Ye *et al.*[10] give a contribution of $\Delta_1^{(4)}(\omega_1)$ to the N-point phonon frequencies which is larger than ours by an order of magnitude. The reason for our result must probably be sought in the inadequateness of our fourth-order anharmonicity, while the third-order part adequately describes the interference effect as discussed in Sec. III E and gives results for $\Delta_1^{(3)}(\omega_1)$ comparable to those of Ye *et al.*[11]

D. Scattering function $S(\mathbf{Q},\omega)$

With the use of $\Gamma(\mathbf{q},\omega)$ and $\Delta(\mathbf{q},\omega)$ we calculate the one-phonon Green function and thus the scattering function $S(\mathbf{Q},\omega)$. As an example, the result for the $L[111]$ branch in bcc Ti at $T=1300$ K is shown in Fig. 8. All spectra are normalized to equal integrated intensity except for $q=0.1$ where it was scaled to fit the maximum intensity. Near the zone center the phonons are only weakly damped. The smallness of the damping and of the shift functions leads to sharp phonon resonances. For higher values of the wave vector the line becomes increasingly broadened, and near $\frac{2}{3}[111]$ we find strongly damped behavior. The comparison with the experimentally observed[1] line shape at $\frac{2}{3}[111]$ shows good agreement. Towards the zone boundary, the lines become sharper again.

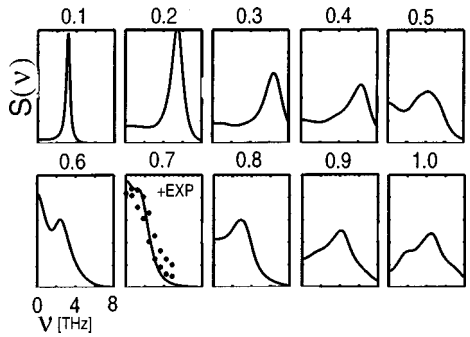

FIG. 8. Scattering functions $S(q,\nu)$ for the longitudinal phonons propagating along [111] in bcc Ti at $T=1300$ K. All spectra except $q=0.1$ are scaled to equal integrated intensity. At $q=0.7$ the experimental data (Ref. 1) are shown.

In the temperature regime around the reference temperature the damping and shift function are proportional to the temperature. Thus, the relative changes of the damping and shift function are equal to the relative temperature changes. This is in agreement with the experiment.

E. Interference effects

The interference effect between one-phonon and multiphonon processes turns out to be small for the first Brillouin zone. For higher values of the scattering vector **Q** the interference effects due to the term H_1 in Eq. (11) become important. The result for the $L\frac{2}{3}$ [111] phonon in bcc Zr for $T=1180$ K at the two symmetrically equivalent points $\zeta=\frac{2}{3}$ and $\zeta=\frac{4}{3}$ is shown in Fig. 9. While the effect on the line shape is small, there is an enormous influence on the scatter-

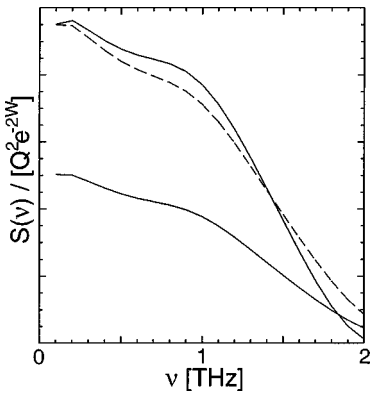

FIG. 9. Reduced neutron-scattering intensity $S(\mathbf{q}+\mathbf{G},\nu)/(e^{-2W(Q)}Q^2)$ in bcc Zr at $T=1180$ K for $\mathbf{q}=\frac{2}{3}(1,1,1)2\pi/a$ with $\mathbf{G}=0$ ($\zeta=\frac{2}{3}$, lower full line) and $\mathbf{G}=(2,2,2)2\pi/a$ ($\zeta=\frac{4}{3}$, upper full line) from two adjacent Brillouin zones. To demonstrate the change in line shape the curve for $\zeta=\frac{2}{3}$ is scaled to the height of the one for $\zeta=\frac{4}{3}$ (broken line).

ing intensity: Apart from the factor $Q^2e^{-2W(\mathbf{Q})}$, which determines the scattering intensity in the harmonic case, we observe a strong intensity variation interference causes additional scattering intensity at $\zeta=\frac{4}{3}$ by a factor of 2 with respect to $\zeta=\frac{2}{3}$. Zhang *et al.*[14] have found a larger anomalous intensity variation, but their line shape is less close to experiment.[4]

In principle, anharmonic contributions to the Debye-Waller factor could lead to an abnormal intensity variation, too. In the case of solid bcc He the anharmonic contributions to the Debye-Waller factor $e^{-2W(\mathbf{Q})}$ amount to less than 2%.[22,23] Simulating the interference effect by an effective Debye-Waller factor[24] is in gross disagreement with this result. Interference between one- and two-phonon processes was able to explain the observed intensity anomalies in bcc He.[23,24] We have therefore refrained from calculating the Debye-Waller factor to higher order in bcc metals because of the expected smallness of the effect.

IV. CONCLUSIONS

The unusual lattice-dynamical and neutron-scattering properties of bcc Zr and bcc Ti can be explained with a simple, central, anharmonic model potential. Its derivatives yield both quasiharmonic and anharmonic force constants and thus the quasiharmonic phonon frequencies and anharmonic self-energies. The anharmonic effects such as line broadening, line shift, and interference are very strong and not just a small correction to the harmonic properties, and they are most important for those phonons whose displacement patterns correspond to the ones towards the transitions to the low-temperature or the high-pressure phase. The lifetime of these phonons is of the order of one vibrational period.

In addition, the so-called symmetry breaking behavior of the neutron-scattering cross section can be explained. Although the bcc structure is the starting point of our calculations, the higher-order derivatives of the potential give rise to the supposed breaking of the bcc symmetry: Slightly different phonon line shapes are observed at equivalent points in different Brillouin zones. This behavior is caused by the interference between one- and two-phonon processes which results in a larger periodicity in reciprocal space as compared with the one-phonon properties. Connected with the interference is an abnormal increase of the scattering intensity beyond the factor $Q^2e^{-2W(\mathbf{Q})}$ (typical of one-phonon scattering processes) for larger values of the scattering vector $\mathbf{Q}$.

ACKNOWLEDGMENTS

The authors are grateful for conversations with W. Petry, J. Neuhaus, W. Schirmacher, K. Nikolaus, and O. Dubos who communicated details of their work and who stimulated this study. The authors are also grateful to the BMBF for the financial support under Contract No. 03ST3REG.

*Present address: Institute Laue-Langevin, B.P. 156, F-38042 Grenoble CEDEX, France; electronic address: tmay@ill.fr

[1] W. Petry, A. Heiming, J. Trampenau, M. Alba, C. Herzig, H. R. Schober, and G. Vogl, Phys. Rev. B **43**, 10 933 (1991).
[2] A. Heiming, W. Petry, J. Trampenau, M. Alba, C. Herzig, H. R. Schober, and G. Vogl, Phys. Rev. B **43**, 10 948 (1991).
[3] F. Güthoff, W. Petry, C. Stassis, A. Heiming, B. Hennion, C. Herzig, and J. Trampenau, Phys. Rev. B **47**, 2563 (1993).
[4] O. Dubos (private communication).
[5] B. V. Thompson, Phys. Rev. **131**, 1420 (1963).
[6] R. A. Cowley and W. J. L. Buyers, J. Phys. C **2**, 2262 (1969).
[7] H. R. Glyde, Can. J. Phys. **52**, 2281 (1974).
[8] J. Meyer, G. Dolling, R. Scherm, and H. R. Glyde, J. Phys. F **6**, 943 (1976).
[9] J. Scheipers and W. Schirmacher, Z. Phys. B **103**, 547 (1997).
[10] K.-M. Ho, C. L. Fu, and B. N. Harmon, Phys. Rev. B **29**, 1575 (1984).
[11] Y. Y. Ye, Y. Chen, K. M. Ho, and B. N. Harmon, Phys. Rev. Lett. **58**, 1769 (1995).
[12] F. Willaime and C. Massobrio, Phys. Rev. B **43**, 11 653 (1991).
[13] S. K. Saxena, S. C. Upadhyaya, J. C. Upadhyaya, R. Shyam, and R. M. Agrawal, Solid State Commun. **99**, 519 (1996).
[14] B. L. Zhang, C. Z. Wang, K. M. Ho, and B. N. Harmon, Phys. Rev. Lett. **74**, 1375 (1995).
[15] Y. N. Gornostyrev, M. I. Katsnelson, A. V. Trefilov, and S. V. Tretjakov, Phys. Rev. B **54**, 3286 (1996).
[16] D. Strauch and T. May, Physica B **219&220**, 396 (1996).
[17] T. May and D. Strauch, Physica B **234–236**, 131 (1997).
[18] A. A. Maradudin and A. E. Fein, Phys. Rev. **128**, 2589 (1962).
[19] H. Bilz, D. Strauch, and R. K. Wehner, in *Handbuch der Physik*, edited by S. Flügge and L. Genzel (Springer, Heidelberg, 1984), Vol. 25/2d.
[20] M. Zoli, G. Santoro, V. Bortolani, A. A. Maradudin, and R. F. Wallis, Phys. Rev. B **41**, 7507 (1990).
[21] J. Trampenau, A. Heiming, W. Petry, M. Alba, C. Herzig, W. Miekeley, and H. R. Schober, Phys. Rev. B **43**, 10 963 (1991).
[22] H. Horner, Z. Phys. **242**, 432 (1971).
[23] H. Horner, Phys. Rev. Lett. **29**, 556 (1972).
[24] E. B. Osgood, V. J. Minkiewicz, T. A. Kitchens, and G. Shirane, Phys. Rev. A **5**, 1537 (1972).